

**Research Article**

**Grain sorting effects on geochemical characteristics of sulfide mine tailings: a case study**

**J.C. Arranz-González<sup>1\*</sup>, V. Cala-Rivero<sup>2</sup>**

<sup>1</sup> Mining Waste Research Group, Geological Survey of Spain. Ríos Rosas, 23, 28003 Madrid, Spain.

<sup>2</sup> Department of Geology and Geochemistry. Faculty of Sciences. Autonomous University of Madrid. 28049 Madrid, Spain.

\*corresponding author: jc.arranz@igme.es

**Abstract:** The geochemical evolution of a sulfide mine tailings impoundment in SW Spain was studied. The impoundment was selected because of its small size and its tailings deposition system with a simple discharge point. The objective of this study was to test the hypothesis that mineral segregation associated to hydraulic sorting has significant effects on the geochemical characteristics and the long term weathering. Tailings samples were collected along depth profiles in three sampling points (proximal, central and distal to the point of discharge), and characterized by color, grain size, pH, acid-base account and chemical elements concentration, with the help of routine XRD analysis. Three vertical zones were identified: an upper oxidized zone, a transition intermediate zone, and an unoxidized zone. The analytical results indicate a segregation pattern in the unoxidized tailings based on differences in size and density of tailings grains. Near the discharge point, tailings were coarser and rich in pyrite, whereas the proportion of silicates increased from proximal to distal points. This results in a clear zoning which has consequences on geochemical and mineralogical evolution under weathering, showing substantial differences in the depth of the oxidation front, the acid generation and neutralization capacity, the formation of Fe secondary phases (jarosite) and the total content of the sulfide-related elements (Fe, As, Zn, Cu, Pb and Cd). The results of the study can serve to improve the theoretical bases for the development of conceptual models for predicting environmental impacts associated with sulfide tailings impoundments. Recently, the impoundment has been covered with a soil cover. This fact offers the possibility of new research on its evolution under new conditions.

**Keywords:** grain sorting, mineral segregation, SW Spain, tailings weathering

**Introduction**

Flotation is the most widespread process for the treatment of base-metal sulfide ores in order to recovery metal concentrates. Grinding may play a key role in controlling the efficiency of mineral flotability, and the selectivity against sulfide gangue mineral components (Grano, 2009). Ideally, the original ore is crushed or ground to a grain size smaller than 0.1 mm in order to release the valuable constituents. Flotation produces fine-grained wastes (sand to silt sized) known as tailings that are normally discharged as slurry to a final storage impoundment. When the tailings are disposed, a segregation process occurs due to hydraulic sorting. This grain-size segregation causes a settling of coarser fractions near the

discharge point, whereas finer fractions settle in distal portions of the impoundment (Robertson,1994). Regarding a specific position of a given impoundment, the vertical layering is not perfectly homogeneous, since it occurs an alternation of different grain-sized tailings (Dold, 2010). Once milling ceases, the tailings dry up, and consolidation and weathering processes take place. Where mine-tailings are exposed to oxygen and water, sulfide oxidation can generate acid mine drainage containing high concentrations of metals. With time, an oxidation front and geochemical zoning are formed. These processes have been quite well studied (e.g.: Blowes and Ptacek, 1994; Holmstrom et al., 1999; Dold and Fontboté, 2001; McGregor and Blowes, 2002; Sidenko et al., 2005, 2007). However, the

influence of sorting on geochemical characteristics of tailings has not yet been systematically studied. The aim of this work was to investigate the different geochemical, physical, and mineralogical changes resulting from weathering in the different parts and layers of a tailings impoundment, under humid Mediterranean climate. The research was focused on the consequences of sulfide oxidation, especially: grain size changes, acid generation, solid-phase partitioning and the secondary minerals formation. The objective was to test the hypothesis that grain sorting has a significant effect on the geochemical characteristics of tailings depending on the position they occupy with respect to the point of discharge. The effects of subsequent long-term weathering are analysed. The results of this study may represent a modest step forward on the development of improved conceptual geochemical models applicable to tailings impoundments. On the other hand, the high levels of some toxic elements and the acidity of the surface layers, have recently led to the current responsible to remedy the dam using a soil cover. The study data were obtained prior to the cover installation. Although some time has passed since then, it has been considered of interest to make them known. The possibility of further research into evolution under these new conditions is open.

## Materials and Methods

### Study area

The study area is located in the proximity of La Nava (Huelva Province, SW Spain; Figure 1). The coordinates are X= 698.650.88 and Y= 4.223.79 (UTM, Zone 29, WGS84). The mine falls within a complex tectono-metamorphic area located in the Ossa-Morena Zone, bordering with the South Portuguese Zone (SW Iberian Massif). The María Luisa massive Cu-Zn sulfide ore deposit is hosted in quartz-sericite schists (probably altered metavolcaniclastic rocks) with some intercalations of amphibolites, calc-silicate hornfelses and metalimestones that were strongly chloritized, silicified and skarnified (Tornos et al., 2004). Vázquez (1972) distinguished two types of ores: an early syngenetic ore, consisting predominantly of pyrite, arsenopyrite and sphalerite, which is overprinted by a late ore with magnetite, pyrrhotite, arsenopyrite, pyrite, sphalerite, chalcocopyrite and galena. The mine was worked for Cu-Zn and pyrite concentrates. The grade of the mineralization was: 0.8% Cu, 3.0% Zn, 0.5% Pb and 50 g/t Ag (Vázquez, 1972). The study area has a Mediterranean humid climate. Annual rainfall is 995 mm and mean temperature is 14.9

°C (data obtained in the nearby Galaroza weather station; X: 701.300, Y: 4.200.105, Zone 29 WG584). Annual potential evapotranspiration value is 750 mm in Galaroza. The dry period, identified with Thornthwaite water balance (Thornthwaite and Mather, 1955, 1957), extends from July to August.



Figure 1. Simplified map showing the location of the studied tailings impoundment. The dashed lines separate different geologic domains (OMZ: Ossa-Morena Zone; SPZ: South Portuguese Zone).

The potential vegetation mainly consists of evergreen oaks (*Quercus rotundifolia* and *Q. suber*) mixed forest. The predominant land use is olive groves and meadows exploited for livestock. The soils are poorly developed: Lithic, Distric and Eutric Leptosols (Junta de Andalucía, 2004). For the available information, it appears that the activity of the impoundment (MALU) ceased in 1979. From that time until recently, when was covered with soil material, the tailings impoundment was subjected to weathering (around 30 years). It is a small facility that covers about 0.2 ha. The thickness of the tailings ranges from less than 1 m to approximately 2.5 m. It is enclosed by a perimeter dyke that surrounds the west and northwest, constructed with materials

excavated in natural ground. The rest of the perimeter is enclosed by cut slopes. The flotation tailings were discharged from the open end of a pipeline approximately from the southeast of the tailings deposit towards the northwest. The underlying bedrock is composed by schists. The impoundment gradually narrows (in depth) from SE to NW, with the exception of an intermediate area.

### **Sampling and field methods**

Three sampling points were selected within tailings impoundment: MALUP (proximal, near the discharge point), MALUC (central) and MALUD (distal). Pit and drill samples were taken in late May, and were preserved in polyethylene bags, transported and processed separately. Color was determined on moist or very moist state, using Munsell® Soil Color Charts. To facilitate profile descriptions, top layers were observed and sampled into trenches excavated with hand shovel to the apparent lower limit of oxidation front. The deepest samples were taken with a split-spoon sampler with a percussion power hammer. This equipment provides cores of tailings in methacrylate tubes. Near the discharge point (MALUP), samples were collected to a depth of approximately 250 cm, and in the distal point (MALUD) the sampling depth was 205 cm. The profile located close to the middle (MALUC) only had a thickness of 75 cm measured in tailings. A total of 27 samples were taken. Samples were labelled with the name of the sampling point and a number: MALUP-1 to MALUP-11, MALUC-1 to MALUC-7, and MALUD-1 to MALUD-9. Depth of the water table was measured in sampling holes using a flexible tape measure (Figure 2).

### **Analytical procedures**

Grain size distribution of tailings samples was measured by standard dry sieving (ASTM 5000 series) for 2-0.063 mm fractions, in combination with a Micromeritis® SediGraph 5100 for <0.063 mm fractions. Grain density ( $\rho_s$ ) was measured with a Micromeritis® AccuPyc™ 1300 helium gas pycnometer. It has preferred to use the term grain for the individual tailings, assuming that can be formed by one or more minerals. Cumulative grain size distribution was employed to calculate  $D_{50}$  and  $D_{90}$  (passing diameter which allow to pass 50% and 90 % of the sample weight, respectively). Paste pH was measured with a Thermo-Orion® pH-meter. The neutralization potential (NP) of tailings was determined by digestion of 2 g of the samples in hot HCl acid, and then titrated with NaOH (Sobek et al., 1978).  $S_{total}$  was determined using a Leco® furnace, and

$S_{sulfate}$  was measured by X-ray fluorescence using a TXRF Extra II spectrometer, after a 0.2 M  $NH_4$ -oxalic, hot, 2 h leach (Dold, 2003). The difference between  $S_{total}$  and  $S_{sulfate}$  represents the  $S_{sulfide}$  content. Acid-generating potential (AP) was estimated multiplying the  $S_{sulfide}$  percentage by a conversion factor of 31.25 (Cravotta et al., 1990). To evaluate the acid generation capacity, the net neutralization potential ( $NNP=NP-AP$ ) were calculated. NNP is a good guide to screening acid potential of samples when NP values are negatives (see below), i.e. oxidized acid producing tailings.

The determination of total element contents was performed using tri-acid digestion ( $HF-HNO_3-HClO_4$ ) (Walsh et al., 1997; Dold and Fontboté, 2001) followed by ICP-MS (inductively coupled plasma-mass spectrometry) analysis using a Perkin-Elmer® ELAN 6000 spectrometer. Additionally, a routine mineral characterization was carried out by X-ray diffraction of powdered dry samples, using a Philips® PW-1700 diffractometer with monochromated  $CuK\alpha$  X-radiation. Data were collected scanning from 3° to 62° 2 $\theta$  with 0.5 s counting time per step. Experimental XRD data was compared to reference patterns to determine what phases was present. Peak areas and d-spacings were calculated using diffractometer software. Semi-quantitative analysis based of the study of peak areas was carried out for unoxidized samples. A sample-to sample estimation of the relative abundance of selected mineral phases was derived by comparison of the peak height of the XRD reflections data (Muncur et al., 2005). For comparison, the intensity of peaks was normalized so that the maximum intensity peak in XRD pattern is 3500 counts per second (cps) according to the following expression:  $R = P_m \times (P_{max}/3500)$ , where R is the relative intensity for the studied mineral (cps);  $P_m$  is the peak intensity in XRD pattern for the studied mineral (cps), and  $P_{max}$  is the peak of maximum intensity in XRD pattern (cps). The maximum peak height intensity always coincided with the value d-spacing = 3.34 Å, that is a typical peak of quartz but not exclusively.

A statistical bivariate analysis was performed using SPSS 13.0 for Windows. A matrix of Pearson's correlation coefficients was examined to identify trends between metals and other chemical and physical properties. Depending of the data, the characteristics for each recognised zones were described in two different ways: the ranges of the results, and/or the weighted average in relation to the thickness of the different layers (hereafter WA).

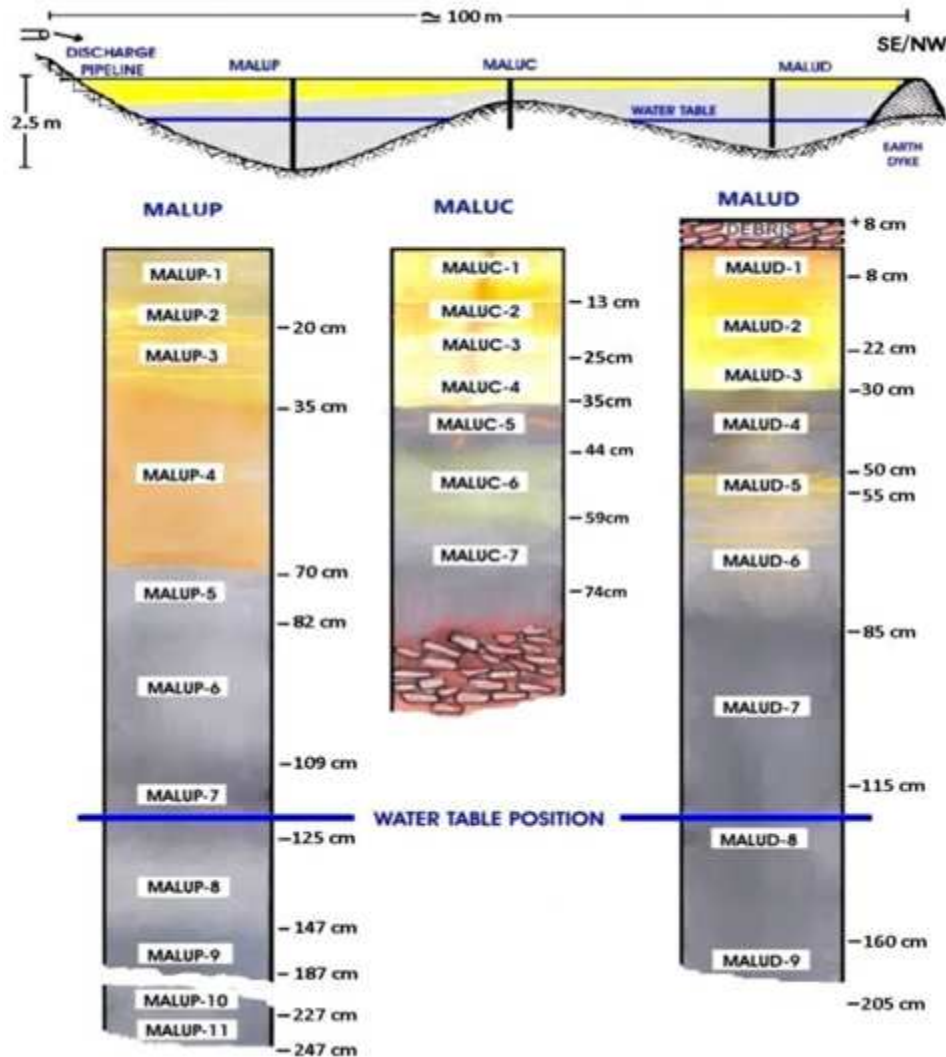


Figure 2. Position of sampling points, schematic cross section and location of samples. The color for each column shows an approximation to the real color. The presence of yellowish to reddish hues, in contrast to grey colors, is an indicator of oxidation processes. The numbers next to the each column indicate the depth in centimeters with respect to the surface of the impoundment.

## Results and Discussion

### *Visual properties in vertical profiles*

In MALU impoundment three vertical zones were identified: an upper oxidized zone (dominated by yellow, brown, and ochre layers), a transition intermediate zone (with a great range of colors: very dark greenish grey, grey silt layers interbedded with thin brown sandy layers, olive yellow sandy layers, brownish cracks, etc.), and a unoxidized zone (dominated by grey and black) (Figure 2; Table 1). The terms oxidized/unoxidized should not be understood as a rigorous chemical oxide-reduction status but rather as a general description of sulfide tailings weathering. The contrasts in color were very visible and easy to distinguish in the test pits.

These color variations are indicative of distinct chemical and mineralogical composition, as described in other tailings studies (e.g.: Dold and Fontboté, 2001; Sidenko et al., 2005, 2007; Hakkou et al., 2008; Parvainen, 2009). It was noted that moisture was increasing from a dry state on surface to a saturated condition (with free water) on MALUC-8 to MALUP-11, and on MALUD-8 and MALUD-9).

### *Physical and mineralogical characterization of unoxidized zone*

In the vicinity of the discharge point (MALUP), a clearly unoxidized deep zone of 122 cm thickness was identified, extending approximately from 125 cm to the bottom of the tailings deposit to a depth of approximately 247 cm depth.

Table 1. Samples description and grain sizes. OX:oxidized zone; TR: transition zone, and UNOX: unoxidized zone. Sand, silt and clay fractions represents respectively: 2-0.063 mm, 0.063-0.002 mm and <0.002 mm. D<sub>50</sub> and D<sub>90</sub> are passing diameter which allow to pass 50% and 90 % of the sample weight, respectively. ρ<sub>S</sub> represents grain density.

Sample	Zone	Thickness (cm)	Color Munsell (field)	Sand/Silt/Clay (wt%)	D <sub>90</sub> (mm)	D <sub>50</sub> (mm)	ρ <sub>S</sub> (Mg/m <sup>3</sup> )
MALUP-1	OX	12-14	Alternating very fine layers 10YR 6/8 and 2.5Y 8/8	27.8/53.2/19.0	0.240	0.020	2.73
MALUP-2	OX	0-5	Variegated of 10YR 6/8, 2.5Y 8/6 and 5GY 7/1	33.8/51.0/15.2	0.220	0.033	2.71
MALUP-3	OX	18-21	Alternating fine layers 5YR 5/8 and 10YR 6/8	50.2/37.5/12.3	0.380	0.063	2.70
MALUP-4	OX	35	Alternating very fine layers 5YR 5/8, 10YR 6/8 and 2.5Y 8/6	47.7/42.2/10.1	0.250	0.054	2.69
MALUP-5	TR	12	5GY 5/1	55.1/41.0/3.9	0.440	0.082	2.93
MALUP-6	TR	27	10GY 4/1	36.1/59.2/4.7	0.130	0.040	2.82
MALUP-7	TR	16	10GY 3/1	12.3/81.5/6.2	0.095	0.017	2.74
MALUP-8	UNOX	22	5G 4/1	57.9/38.8/3.3	0.380	0.090	3.16
MALUP-9	UNOX	40	5G 3/1	57.4/39.9/2.7	0.340	0.081	3.14
MALUP-10	UNOX	40	5G 3/1	68.7/29.7/1.6	0.380	0.110	3.31
MALUP-11	UNOX	20	5G 3/1	73.6/24.3/1.1	0.690	0.165	3.14
MALUC-1	OX	12-14	Alternating very fine layers 7.5YR 5/8, 10YR 3/6 and 5Y 7/4	6.0/79.6/14.4	0.058	0.011	2.63
MALUC-2	OX	9	10YR 5/6,	48.9/42.6/8.5	0.190	0.057	2.68
MALUC-3	OX	2-4	5Y 7/3 with cracks 7.5YR 5/8	5.7/83.2/11.1	0.052	0.013	2.60
MALUC-4	OX	10	Variegated of 10YR 5/6, 2.5Y 6/6, with fine layers 5Y 7/3 and cracks 10YR 5/6	36.5/53.9/9.6	0.155	0.035	2.67
MALUC-5	TR	9	5GY 5/1, with crack 2.5Y 6/6 and lens 2.5Y 6/6	2.2/91.6/6.2	0.038	0.013	2.63
MALUC-6	TR	15	Variegated of 2.5Y 7/4 and 10YR 5/6	21.1/68.3/10.6	0.096	0.022	2.64
MALUC-7	UNOX	15	5Y 3/2	45.2/49.8/5.0	0.187	0.046	2.84
MALUD-1	OX	8	Alternating very fine layers 7.5YR 4/3 and 2.5Y 6/6	33.5/54.3/12.2	0.165	0.011	2.71
MALUD-2	OX	14	2.5Y 6/6	9.8/67.9/22.3	0.060	0.013	2.71
MALUD-3	OX	8	Alternating very fine layers 7.5YR 3/4, 10YR 4/6 and N 2.5/1	13.1/66.6/20.3	0.075	0.012	2.75
MALUD-4	TR	20	Alternating very fine layers N 2.5/1, 7.5YR 3/4 and 10YR 4/6	5.3/85.4/9.3	0.043	0.011	2.84
MALUD-5	TR	5	Variegated of 5Y 6/6 and 2.5Y 6/8	1.3/90.3/8.4	0.036	0.023	2.71
MALUD-6	TR	30	N 4/1 with fine layers 10YR 6/6 and 7.5Y 4/6	25.2/63.6/11.2	0.100	0.013	2.79
MALUD-7	UNOX	30	N 4/1 with few fine layers 10YR 6/6 and 7.5Y 4/6	5.6/90.4/4.0	0.042	0.017	2.83
MALUD-8	UNOX	45	N 4/1	14.0/80.3/5.7	0.078	0.012	2.95
MALUD-9	UNOX	45	N 4/1	3.2/88.1/8.7	0.057	0.016	2.94

Within this zone, the deepest layers were very dark greenish gray (5G 4/1 or 5G 3/1). Unoxidized tailings were identified to a thickness of 120 cm (from a depth of 85 to 205 cm) in the distal point (MALUD) (Table 1; Figure 2). The color of this zone was black (N 4/1). Gray uniform layers were poorly represented in the central location of the impoundment (MALUC) due to the shallowness of the bottom at this location. The thickness of this layer was approximately 15 cm (59-74 cm depth). The color of unoxidized tailings at this point (MALUC-7) was dark olive gray (5Y 3/2). The grain size of unoxidized tailings was progressively finer when distance from the discharge point increases. It was classified as loamy sand, loam and silty for the

proximal, central and distal points respectively. Considering  $D_{50}$  and  $D_{90}$ , the WA of  $D_{50}$  was: 0.106 mm for proximal (range 0.081 to 0.165 mm), 0.046 mm for central (only one sample), and 0.014 mm (range 0.012 to 0.017 mm) for distal. The WA of  $D_{90}$  was: 0.418 mm (range 0.340-0.690 mm) for proximal, 0.187 mm for central, and 0.060 mm (range 0.042-0.078 mm) for distal samples. Such data indicate that there is a segregation of grain-size from MALUP to MALUD, with a remarkable increase of finer fractions (Figure 3) related to the decrease of hydrodynamic energy from the original discharge point. Similarly, as a result of this segregation, the permeability of tailings will decrease with increasing distance to the discharge point.

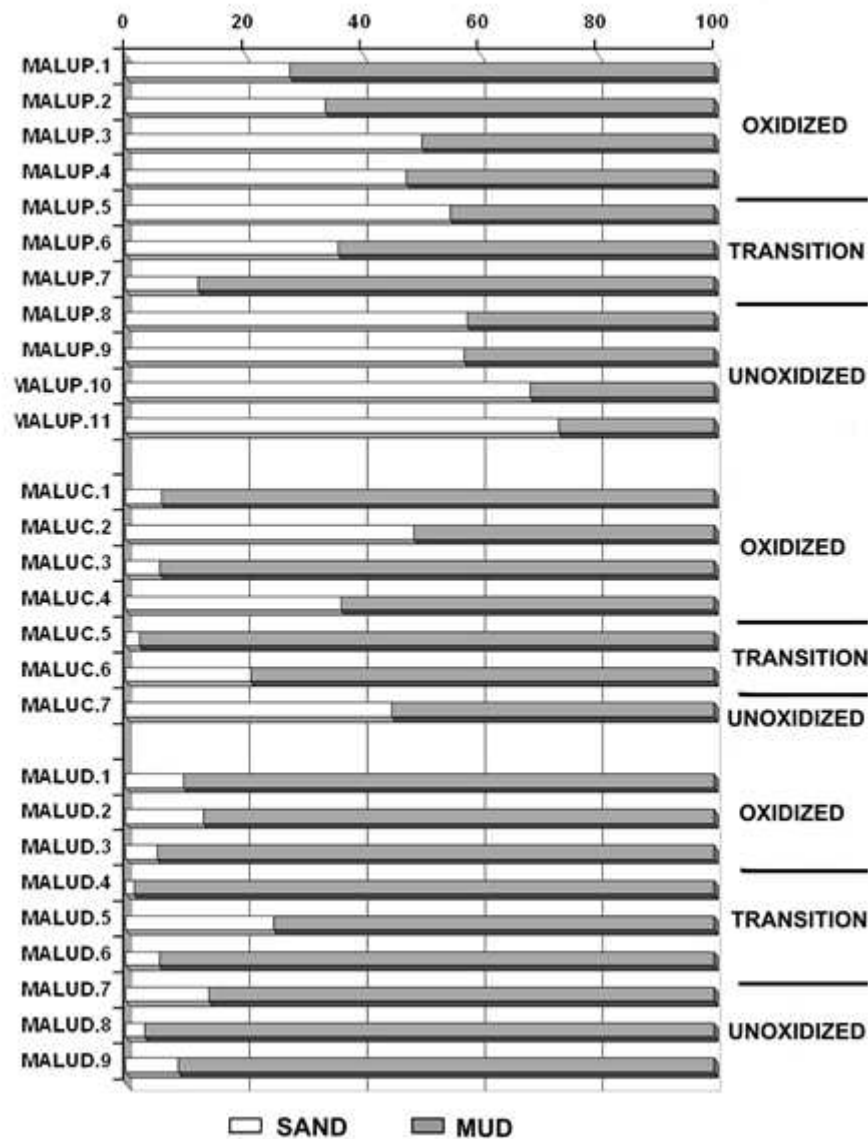


Figure 3. Grain-size fraction percentage of the samples obtained from MALUP, MALUC and MALUD profiles: sand (2-0.063 mm) and mud (silt + clay: <0.063 mm).

Quartz, chlorite [ferroan clinocllore:  $(Mg, Fe)_3(Si, Al)_4O_{10}(OH)_2(Mg, Fe)_3(OH)_6$ ], oligoclase  $[(Na,Ca)(Al,Si)_4O_8]$ , muscovite  $[KAl_2(Si_3,Al)O_{10}(OH)_2]$ , riebeckite  $[Na_2(Fe, Mg)_3Fe_2Si_8O_{22}(OH)_2]$ , pyrite  $[FeS_2]$ , sphalerite  $[(Zn, Fe)S]$ , galena  $[PbS]$ , chalcopyrite  $[CuFeS_2]$ , calcite  $[CO_3Ca]$  and gypsum  $[CaSO_4 \cdot 2H_2O]$  were the minerals detected by XRD analysis in the unoxidized tailings, although the relative abundance throughout the different areas of the impoundment was variable. The mineralogical XRD results are summarized in Table 2. The constituent minerals were classified as major, moderate, minor and trace depending on their

concentrations. The presence of calcite as trace mineral only in the unoxidized distal tailings can be due to the incorporation of materials from some intercalations of metalimestones in host rocks or as a result of residual traces of carbonate minerals present in lime added during flotation. The results showed in Table 2 and Figure 4 illustrate the mineralogical distribution from proximal to distal points. In the proximal point the major metal mineral was pyrite. With increasing distance from the discharge point, the pyrite concentration decreases, whereas concentration of silicates increase.

Table 2. Semi-quantitative mineralogical analysis by XRD in unoxidized raw tailings.

	<b>Major</b>	<b>Moderate</b>	<b>Minor</b>	<b>Traces</b>
MALUP	Quartz , pyrite	Chlorite, muscovite	Oligoclase, riebeckite	Chalcopyrite
MALUC	Quartz	Oligoclase, chlorite muscovite	Pyrite, riebeckite	
MALUD	Quartz, chlorite	Muscovite, riebeckite	Pyrite	Sphalerite, galena, calcite

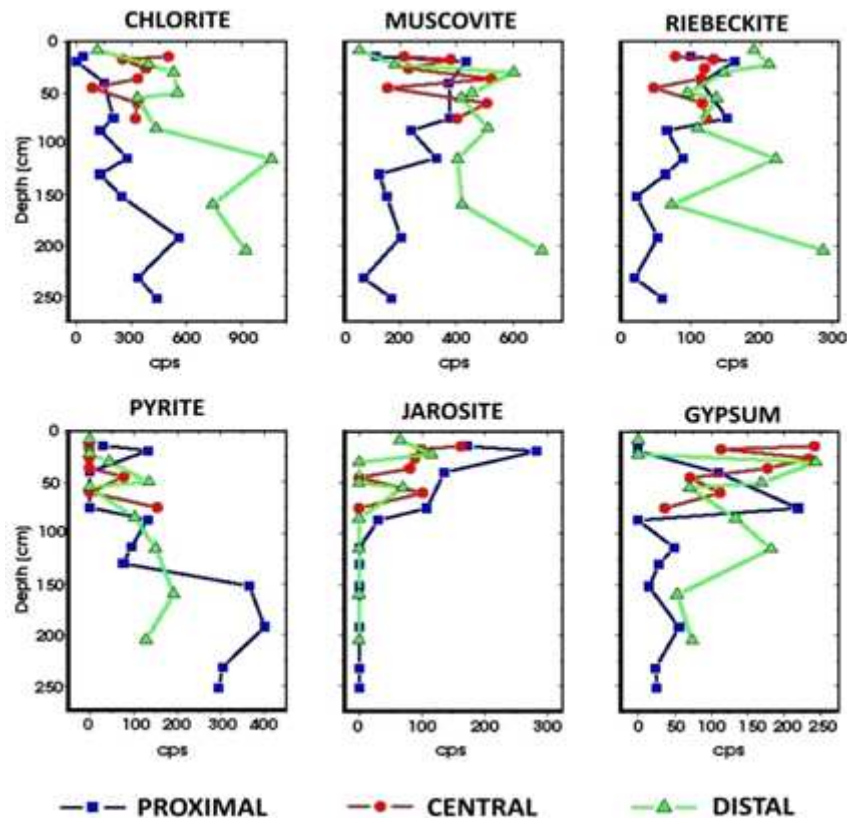


Figure 4. Distribution of minerals versus sampling depth for proximal, central, and distal points. Scale on the x axis corresponds to the comparison of peak height of a specific X-ray reflection as a tool to evaluate the relative abundance (based on Moncur et al., 2005).

Sphalerite and galena only appear at trace concentrations in distal point. On the contrary, chalcopyrite is only present in proximal samples. This mineralogical differentiation is related to physical segregation of the tailings particles. Using the Stokes law is possible to explain that the more dense and of greater size (or both) tend to settle in proximal points. Indeed, the grain density of the proximal unoxidized tailings (3.14-3.31 Mg/m<sup>3</sup>) was greater than of central sample (2.84 Mg/m<sup>3</sup>) or the distal tailings (2.83-2.95 Mg/m<sup>3</sup>). Pyrite density (5.01 Mg/m<sup>3</sup>) is greater than that of silicate gangue minerals: muscovite (2.88 Mg/m<sup>3</sup>), chlorite (3.02 Mg/m<sup>3</sup>), riebeckite (3.44 Mg/m<sup>3</sup>) and albite (2.65 Mg/m<sup>3</sup>), confirming that the tailings density results (Table 1) were clearly related with mineral constitution. Therefore, the differences in density of the unoxidized tailings, together with differences in grain size, lead to the preferential deposition of pyrite near the discharge point, whereas silicates can be transported further.

The appearance of galena (with a density of 7.5 Mg/m<sup>3</sup>) in the distal samples can only be explained because the grinding method pulverizes it to a greater degree than other minerals. The separation of sphalerite (4.09-4.1 Mg/m<sup>3</sup>) and chalcopyrite (4.1-4.3 Mg/m<sup>3</sup>) may be a consequence of ore structure, milling and flotation, but existing data are insufficient to explain it.

#### Geochemical characterization of unoxidized zone

The chemical analysis and pH values of the tailings are shown in Tables 3 and 4. Only the deepest samples of MALUD are neutral to slightly alkaline based on paste pH values (Table 3). Calcite in the distal and deepest unoxidized zone has likely contributed to raise higher pH values (5.06 to 7.34). The rest of unoxidized samples are strong acid (values in the range between 3.39 and 3.60).

Table 3. pH, sulphur forms, and acid-base account. OX means oxidized zone; TR means transition zone, and UNOX means unoxidized zone. Neutralization potential (NP), acid potential (AP), and calculated net neutralization potential (NNP=NP-AP) in kg CaCO<sub>3</sub>equivalent/1000 t. AP is estimated multiplying wt% S<sub>sulfide</sub> by 31.25.

Sample	Zone	pH	wt% S <sub>total</sub>	wt %S <sub>sulfate</sub>	wt% S <sub>sulfide</sub>	NP	AP	NNP
MALUP-1	OX	1.86	4.25	3.62	0.63	-11.3	19.7	-31.0
MALUP-2	OX	1.79	4.65	4.50	0.15	-19.2	4.7	-23.9
MALUP-3	OX	2.19	3.48	3.30	0.18	-18.7	5.6	-24.3
MALUP-4	OX	2.30	2.67	2.58	0.09	-13.2	2.8	-16.0
MALUP-5	TR	3.24	5.80	0.72	5.08	+27.4	158.8	-131.4
MALUP-6	TR	3.46	5.85	0.86	4.99	-7.8	155.9	-163.7
MALUP-7	TR	3.33	3.97	0.96	3.01	+11.7	94.1	-82.4
MALUP-8	UNOX	3.56	12.60	0.31	12.29	+8.2	384.1	-375.9
MALUP-9	UNOX	3.39	19.70	0.52	19.18	+33.1	599.4	-566.3
MALUP-10	UNOX	3.40	23.20	0.57	22.63	+9.8	707.2	-697.4
MALUP-11	UNOX	3.60	21.70	0.34	21.36	+3.5	667.5	-664.0
MALUC-1	OX	2.96	3.93	3.25	0.68	-17.9	21.3	-39.2
MALUC-2	OX	3.17	1.72	1.69	0.03	-4.0	0.9	-4.9
MALUC-3	OX	2.87	1.75	1.70	0.05	-15.3	1.6	-16.9
MALUC-4	OX	3.03	1.71	1.18	0.53	-4.9	16.6	-21.5
MALUC-5	TR	3.19	3.88	1.36	2.52	-14.4	78.8	-93.2
MALUC-6	TR	2.73	2.16	1.97	0.19	-10.8	5.9	-16.7
MALUC-7	UNOX	3.52	5.60	0.79	4.81	-7.2	150.3	-157.5
MALUD-1	OX	3.19	2.00	2.25	---	-1.7	0.0	-1.7
MALUD-2	OX	3.20	1.98	2.10	---	-4.0	0.0	-4.0
MALUD-3	OX	3.25	2.04	1.98	0.06	-1.2	1.9	-3.1
MALUD-4	TR	3.58	4.89	0.79	4.10	-2.7	128.1	-130.8
MALUD-5	TR	3.24	1.33	1.30	0.03	-1.0	0.9	-1.9
MALUD-6	TR	4.09	2.56	0.14	2.42	+6.19	75.6	-69.4
MALUD-7	UNOX	5.06	3.80	0.41	3.39	+7.07	105.9	-98.9
MALUD-8	UNOX	7.17	4.46	0.13	4.33	+25.5	135.3	-109.8
MALUD-9	UNOX	7.34	3.89	0.16	3.73	+27.4	116.6	-89.2

Table 4. Concentrations of Ca, Mg, Na, K, Fe and Al (expressed in wt.%) and As, Cd, Cu, Pb and Zn (expressed in mg/kg) in the studied tailings profiles.

<b>Sample</b>	<b>Ca</b>	<b>Mg</b>	<b>Na</b>	<b>K</b>	<b>Fe</b>	<b>Al</b>	<b>As</b>	<b>Cd</b>	<b>Cu</b>	<b>Pb</b>	<b>Zn</b>
MALUP-1	0.34	0.32	0.73	2.22	7.43	0.92	72.34	0.34	1980.96	703.47	417.00
MALUP-2	0.27	0.23	0.62	2.64	7.41	1.28	56.50	8.13	1733.10	2117.00	342.11
MALUP-3	1.45	0.98	1.29	4.87	7.97	2.57	47.80	0.14	629.00	751.05	379.00
MALUP-4	1.62	1.02	1.39	4.25	8.57	2.21	44.18	0.19	704.36	748.45	404.11
MALUP-5	0.28	1.80	0.99	2.43	5.03	2.51	22.13	78.30	5268.40	1672.90	21747.47
MALUP-6	1.42	2.59	1.50	5.28	6.26	4.78	29.38	514.19	4386.85	1529.74	20855.93
MALUP-7	1.12	2.04	1.13	4.85	4.96	4.32	28.96	332.40	929.49	2104.61	13321.49
MALUP-8	0.64	1.23	0.43	2.41	8.78	1.89	72.52	67.52	3272.02	1391.47	12348.58
MALUP-9	0.45	1.23	0.33	1.24	11.10	1.71	69.88	15.56	1818.87	1071.01	4905.93
MALUP-10	0.65	1.39	0.25	0.96	14.63	1.77	71.98	24.58	3088.93	1082.53	7626.31
MALUP-11	0.85	1.04	0.45	3.14	9.57	1.70	58.81	29.58	3296.99	779.37	6799.63
MALUC-1	1.47	1.35	0.44	3.25	5.64	2.04	34.47	11.07	1098.94	2269.53	2504.80
MALUC-2	1.34	1.71	1.45	4.71	6.17	3.07	29.52	3.58	853.61	565.04	1083.03
MALUC-3	1.48	2.26	0.78	4.71	3.98	3.29	29.09	26.46	763.96	690.26	3708.05
MALUC-4	1.32	1.98	1.41	5.40	5.90	3.22	20.92	7.40	779.81	801.75	1933.49
MALUC-5	0.97	3.20	1.01	6.42	4.83	4.64	21.44	4.70	5349.49	866.40	12020.01
MALUC-6	0.92	1.84	0.99	4.77	5.52	2.65	21.56	11.00	507.82	784.37	2038.95
MALUC-7	1.13	2.72	0.98	4.69	4.98	4.59	42.14	57.45	1225.32	3108.23	15991.87
MALUD-1	1.04	1.48	0.96	3.33	7.51	4.36	62.20	0.89	598.26	1170.85	441.66
MALUD-2	0.71	1.43	0.99	3.95	9.85	2.40	71.48	0.81	465.58	894.09	423.77
MALUD-3	1.46	2.24	0.67	1.20	6.56	3.40	113.35	10.92	2634.34	570.43	4840.44
MALUD-4	1.15	2.16	0.46	4.32	5.25	3.72	57.79	46.33	4684.06	12116.85	6662.06
MALUD-5	1.04	2.24	1.31	5.49	6.53	3.27	38.90	0.45	313.23	658.38	727.28
MALUD-6	1.00	2.84	0.72	5.21	4.57	3.76	22.28	23.74	403.56	2325.40	4248.47
MALUD-7	1.23	4.72	1.04	5.96	5.39	4.92	32.25	93.25	1449.62	4968.94	25177.41
MALUD-8	1.08	2.86	0.22	0.21	5.75	2.58	40.32	135.04	2060.84	4302.50	33068.10
MALUD-9	1.55	3.48	0.40	0.44	4.85	3.53	56.76	141.98	2321.54	5543.11	33888.77

The results of AP were in accordance with pyrite segregation from proximal to distal positions. Since it is known, chalcopyrite, sphalerite and galena produce acid when ferric iron is the oxidant (Dold, 2010), but the contribution of these minerals is comparatively much less important than pyrite in acid generation. According to Ferguson and Morin (1991), a material can be considered acid generating when its net neutralization potential (NNP) is lesser than -20 kgCaCO<sub>3</sub> equivalent/t. Applying these criteria, all the unoxidized tailings could be considered acid generating (Table 3). The order for NNP values in the tailings was: proximal (-376 to-697 kg CaCO<sub>3</sub> equivalent/t) << central (-157 kg CaCO<sub>3</sub> equivalent/t) < distal (-89 and -110 kg CaCO<sub>3</sub> equivalent/t). The above tendency can be explained by a progressive decrease in pyrite from the discharge point to the distal point and the slightly higher neutralization potential (NP) of the distal tailings due to the smaller grain-size, the presence of calcite, and the enrichment of aluminosilicates like chlorite. The distribution of total concentrations of selected major and trace elements is shown in the Table 4. The geochemical composition of the unoxidized samples is consistent with the mineralogical data. The proximal unoxidized tailings showed the highest total S (12.6-23.2 wt%) (Table 3) and Fe (8.8-14.6 wt%) (Table 4), which confirms the accumulation of pyrite at the proximal zone to the discharge point (Table 3 and Figure 4), without excluding a comparatively small contribution of chalcopyrite. Fe was positively correlated with As (at p<0.05) suggesting the association of As to pyrite (Blanchard et al. 2007) or to arsenopyrite (FeAsS) although this mineral was not detected by XRD analysis. Arsenopyrite has a high density (6.07 g/cm<sup>3</sup>) and for this reason it would tend to accumulate with the proximal coarser tailings. Fe and As are significantly correlated with density at p<0.05 level, with sand at p<0.05 level and negative correlated at p<0.05 level with silt, confirming their preferential accumulation in the proximal point. Unoxidized samples from the distal point were rich in Al (2.6-4.9%), Mg (2.8-4.7%), Zn (25177- 33889 mg/kg), and Pb (4302-5543) which is consistent with the elevated concentration of aluminosilicates (i.e. chlorite) and the presence of traces of sphalerite and galena (Table 2). Zn was significantly correlated at p<0.01 level with Cd (metal usually present in solid solution with Zn in sphalerite), and with silt and clay fractions, confirming the presence of sphalerite in the finer tailings. The lower concentration of Fe at the distal tailings (4,85-5,75%) is consistent with the presence of pyrite in these tailings as minor mineral (Table 2). Observing the data referring to the thickness-

weighted average metal concentrations, it is clear to appreciate that Fe and As tend to be larger in proximal position, and Zn, Pb and Cd are larger in the distal point (Table 5).

**Physical and mineralogical characterization of oxidized and transition zones**

More than thirty years of weathering of the tailings have generated an oxidized zone which thickness is clearly related to the grain sorting and concentration of pyrite in the unoxidized tailings. The oxidized zone extends from the surface to approximately 70, 35 and 30 cm in the proximal, central and distal points respectively. Below the oxidation zone it appears a transition zone that overlies the unoxidized tailings. The transition zone contains a series of layers with intermediate characteristics where changes and movements were probably more intense at present.

Table 5. Thickness weighted average of selected elements concentrations in unoxidized tailings.

	Proximal	Central	Distal
Fe (%)	9.9	5.0	5.4
As (mg/kg)	59.5	42,1	44,5
Cd (mg/kg)	25.9	57.5	44.5
Cu (mg/kg)	2353.6	1225.3	2005.8
Pb (mg/kg)	931.8	3108.2	4934.3
Zn (mg/kg)	6401.0	15991.9	31403.2

The proximal oxidized zone is visualized (Table 1) as very fine alternating layers in reddish yellow to yellow color (Munsell hue: 5YR-10YR-2.5Y). In the central and distal points the Munsell hue 5YR was no longer visible. Here, the color varied from reddish yellow to olive yellow (Munsell hue: 7.5YR-10YR-2.5Y-5Y) in fine layers, or variegated colors, with brown cracks (7.5YR 5/8). The bottom of the oxidized distal zone was characterized by the presence of very fine black layers (N2.5/1). Below these oxidized layers, the proximal transition zone (70 to 125 cm depth) consists of tailings in which a greenish grey color gradually changes with increasing depth to a dark greenish grey color (Munsell hues: 5GY-10GY). In the central point (approximately 35 to 59 cm depth) and the distal point (around 30 to 85 cm depth), the transition zone is more heterogeneous, consisting of grey silty layers interbedded with thin (<1 cm) brown layers, thick sequences of olive yellow sands and silty dark grey with cracks (10YR-7.5YR-2.5Y-5Y). Close to these cracks, tailings showed yellow and brown colors. The presence of pale yellow layers (5Y 7/3) was remarkable in the central transition zone, whereas black layers (N4/1) were found in the distal

transition zone (Table 1). Oxidized and transition samples are predominantly loam to silt-loam in the proximal point, and loam to silt in central and distal points (Table 1, Figure 3). As a result of the exposition of the surface of tailings to oxidation and weathering, it is evidenced a significant decreasing of the grain size regarding unoxidized tailings. This is particularly true in proximal oxidized layers (with reduction of 57 wt% in  $D_{50}$  and 42 wt% in  $D_{90}$ , on the basis of WA), and in central oxidized layers (decreasing of 50 wt% in  $D_{50}$  and 47 wt% in  $D_{90}$ , on the basis of WA). In the finest distal tailings this reduction was negligible. This fact is attributable to the sulfide oxidation and acid-neutralization processes which entail the breakdown of minerals (Dold and Fontboté 2001), and by the formation of fine sized weathering products. The strong weathering also attenuates the variations in grain density, which was uniform in all oxidized and transition samples (2.60-2.93  $Mg/m^3$ ). Oxidation reactions have resulted in the almost total depletion of sulfide minerals in the upper layers of the oxidized zone along the impoundment. In the absence of suitable acid-neutralizing minerals such as carbonates, the main neutralizing minerals are aluminosilicates, mainly chlorite, but these have a limited acid-neutralization capacity. The acidity released from sulfide oxidation has depleted almost all chlorite and muscovite in the upper 20 cm of the proximal tailings. In these upper layers a transformation of chlorite to interstratified vermiculite-smectite was detected by XRD analysis. Brand et al. (2003) reported the transformation of chlorite into interstratified vermiculite/smectite by the preferential leaching of certain cations from the chlorite structure under acidic conditions. Chlorite and muscovite were also highly depleted from the top 8 cm layer of distal point. This effect was not found in the upper central zone. Jarosite ( $KFe_3(SO_4)_2(OH)_6$ ) and gypsum ( $CaSO_4 \cdot 2H_2O$ ) were the most prominent secondary minerals detected in the oxidized zones of the impoundment (Figure 4). Jarosite was observed throughout the oxidation zone of the tailings as well as in the transition zones of the central and distal tailings. In transition samples of central and distal points, jarosite must be preferentially associated with cracks. Acid fluids from sulfide oxidation can attack muscovite releasing  $K^+$  which is then available to form jarosite. Formation of jarosite requires high levels of  $Fe^{3+}$  and sulfate, acidic ( $pH < 3$ ) and oxidizing environments (Jambor, 1994). Such conditions occurred preferentially in the proximal oxidized zone. XRD analysis indicates a greater amount of jarosite in the proximal zone, which decreases progressively with the increase of the distance to the discharge point (Figure 4). Gypsum was

detected by XRD analysis at the deeper layers of proximal (35 to 70 cm depth) and distal oxidized tailings (25 to 35 cm depth), and at virtually all the central samples, especially below the top 20 cm, which may be a consequence of the precipitation from Ca and sulfate leached from the upper layers. Calcium is released mainly from plagioclases alteration. It is not ruled out that this central zone is slightly depressed with respect to the rest, and may be a zone of surface accumulation of water. This may indicate special conditions of this central part of the impoundment. It is possible that supersaturation processes controls the precipitation of water soluble secondary salts as gypsum ( $CaSO_4 \cdot 2H_2O$ ), detected by XRD analysis, and probably undetected sulfate minerals in this central oxidized zone. The transition zone is generally composed of silty green-gray tailings. As mentioned above, in the central and distal points, the transition zone showed a higher heterogeneity, consisting of grey silt layers interbedded with thin brown layers, thick sequences of olive yellow oxidized sands, or silty dark grey with cracks. This transition zone is probably the most affected by seasonal water table fluctuations. However, some samples in the central and distal tailings (MALUC-6 and MALUD-5) tailings show an olive yellow to yellowish brown color. XRD analysis confirmed the presence of jarosite in these two samples, which suggests that sulfide oxidation is triggered along cracks.

#### ***Geochemical characterization of oxidized and transition zones***

The oxidation of pyrite is the key process controlling the changes in pH, acid-neutralizing capacity due to the dissolution of aluminosilicates and in the concentration and distribution of macro and trace elements within the tailings. The pH values of the oxidized proximal samples are strongly acidic (range 1.79 to 2.30) and progressively increase with increased distance to the original discharge point, ranging from 2.87 to 3.17, and from 3.19 to 3.25 in the central and distal oxidized tailings, respectively. This low pH values are typical of environments with high acid generation potential and low neutralizing capacity, especially near the proximal point. No clear trend could be identified within the transition samples which all have similar pH values ranging from 3.24 to 4.09. The neutralization potential of all the oxidized tailings (NP) was negative, which means that the samples contain residual weathering products that produce acidity upon dissolution. The same applies to the transition samples with the exception of MALUP-5, MALUP-7 and MALUD-6, which are similar to

unoxidized samples (gray to black color). Acid-base accounting results (Table 3) show that most proximal and central oxidized/transition samples can be considered acid-generating as their NNP values are generally less than -20 kg CaCO<sub>3</sub> equivalent/t (Ferguson and Morin 1991). Some oxidized and transition samples (MALUP-4, MALUC-2, MALUC-3, MALUD-1, MALUD-2, MALUD-3 and MALUD-5) produce NNP values that fall in the uncertainty range between acid-generating and non-acid-generating (from -20 to 20 kg CaCO<sub>3</sub> equivalent/t). In the light of all this, it would appear that tailings are less predisposed to generate acid if they are located further away from the discharge point. The oxidation of sulfides and the dissolution of aluminosilicate minerals in the oxidized zone releases sulfate and metals into the tailings pore waters. The metals released could be subsequently attenuated by precipitation, co-precipitation or adsorption into secondary mineral phases (Dold et al. 2001).

A large amount of Al, Ca, Mg, Na and K released by the aluminosilicate dissolution was mobilized from the upper to the deeper oxidized levels of the proximal tailings, as a result of the strong acidity derived from pyrite oxidation and the higher permeability of these coarser layers that enhances the leaching intensity. In oxidized distal tailings these metals don't exhibit this behavior due to the lower sulfide contents available for oxidation and consequently the lower aluminosilicate alteration and the finer texture of these tailings. In the oxidized tailings Fe generated by pyrite oxidation was immobilized in jarosite (Figure 4) and/or secondary Fe-oxy-hydroxides not detected by XRD analysis, decreasing their mobilization to the transition zone. Considering the abundance pattern, both Fe and As exhibit the same behavior. Indeed, the highest concentrations of As were identified in the oxidized zone probably as consequence of the adsorption to the Fe (III)-oxides and/or their incorporation into well-crystallized jarosite. Jarosite group minerals are able to accommodate significant proportions of As by sulfur replacement in sulfate tetrahedral sites (Savage et al., 2005; Paktunc and Dutrizak 2003). Nevertheless, It can be seen an enrichment layer (Table 3) immediately below the more oxidized layers, comprising: MALUP-5, MALUP-6, MALUC-5 and MALUD-4. This could indicate transport of mobilized elements (Cd, Cu, Pb and Zn) from the oxidized zone downwards with percolating water and formation of enriched layers in which these elements may be associated with secondary minerals. In the proximal point this enrichment is absolute, whereas in the other points it is only relative to the oxidized zone. It cannot be ruled out that there has been an

enrichment of Cd and Zn in unoxidized layers of the distal point. The percolation processes can move these highly soluble elements to the unoxidized layers, where immobilization onto sulfides could occur. If the concentrations of Cd, Cu, Pb and Zn are compared for the oxidized and unoxidized layers, it is observed that they are lower in the oxidized layers. This can mean losses, which have been produced over time by deep percolation of the most soluble elements. Apparently, as regards the contents of selected elements, the weathering generates a homogenization between the proximal and distal points, reducing the differences caused by the grain sorting (Table 5 and Table 6).

Table 6. Weighted average of total elemental concentrations in oxidized tailings.

	<b>Proximal</b>	<b>Central</b>	<b>Distal</b>
Fe (%)	8.2	5.5	8.4
As (mg/kg)	50.9	28.9	80.2
Cd (mg/kg)	0.49	9.2	3.5
Cu (mg/kg)	853.9	916.0	1079.3
Pb (mg/kg)	666.3	1276.5	881.6
Zn (mg/kg)	397.3	2023.8	1606.3

The arsenic content of MALUD (113.4 mg/kg) is an anomaly to which no explanation has been found. On the other hand, the total metal concentrations in the two most superficial layers of tailings (≈20 cm) were very high for Cu (598-1981 mg/kg), Pb (565-2269 mg/kg), and Zn (342-2505 mg/kg), and high for As (29-72 mg/kg), if compared with to the 95th percentile for upper soil (0–20 cm) in the geological dominium Ossa Morena Zone (Junta de Andalucía, 2004): 49, 108, 94, and 226 mg/kg, respectively for As, Cu, Pb, and Zn. The surface measured concentrations of these elements and Cd also exceed the values established for soils above which cropping may be unsafe (Kloke, 1979; Kabata Pendias and Pendias, 1984): 20 mg/kg (As), 3 mg/kg (Cd), 100mg/kg (Cu), 100 mg/kg (Pb) and 300 mg/kg (Zn). Despite this, no legally binding obligations existed for this mine, considering that it has worked prior to the promulgation of environmental normative for abandoned mines. However, at some moment, those responsible for the mine considered it necessary to establish a soil cover, in order to minimize possible impacts on the environment. The cover with selected soil material aims to ensure that tailings are not exposed to surface erosion and weathering. A interesting plant colonization and succession have been initiated (Figure 5), which can provide new possibilities for study.



Figure 5. Top: the surface of the tailings impoundment in 2006. Bottom: the tailings impoundment in 2014, showing the colonization of local vegetation over the soil cover.

## Conclusions

In the Maria Luisa tailings impoundment, a clear pattern of grain size segregation was evidenced, as a consequence of the discharge of tailings from a single point. Sorting was mainly due to the density and grain-size of the tailings. Weathering under humid Mediterranean climate was superimposed to this segregation. Three vertical zones were identified: an upper oxidized zone (dominated by yellow, brown and ochre layers), a transition intermediate zone (with a great range of colors that vary from very dark greenish grey to olive yellow, with presence of brownish cracks), and a unoxidized zone (dominated by grey and black). As a consequence of sorting, near the discharge point, unoxidized tailings were coarser and rich in pyrite, whereas the proportion of silicates increased from proximal to distal points. As a result, acid generating potential decreased with increase distance from the discharge point, which in turns had consequences on geochemical and mineralogical evolution under weathering. The oxidation processes that took place caused substantial differences of the depth of the oxidation front and a differential reduction of grain-size. Oxidation reactions have resulted in the almost total depletion of sulfide minerals in the oxidized zone, and the presence of secondary Fe (oxy)hydroxides and well-crystallized jarosite, mainly formed under the more acidic conditions of the proximal oxidized tailings. The results of

this study highlight that grain size segregation can have major implications on geochemical and mineralogical characteristics of the tailings dumped into an impoundment. This process can be magnified in larger impoundments, and consequently the influence of sorting on geochemical and mineralogical zoning must be taken into account for the implementation of effective remediation practices. In this respect, the results of this study could represent a contribution on the development of better conceptual models for predicting environmental impacts associated with closed/abandoned tailings impoundments.

## Acknowledgements

The study was made under financial resources allocated to 542L Program, budget chapter 20-206-640, provided by the Geological Survey of Spain (Instituto Geológico y Minero de España, IGME).

## References

- Blanchard, M., Alfredsson, M., Brodholt, J., Wright, K., Richard, C., Catlow, A. 2007. Arsenic incorporation into FeS<sub>2</sub> pyrite and its influence on dissolution: A DFT study. *Geochimica et Cosmochimica Acta* 71:624–630.
- Blowes, D.W., Ptacek, C.J. 1994. Acid-neutralization mechanisms in inactive mine tailings. In: Jambor JL, Blowes D.W. (Eds.) *Environmental Geochemistry of Sulfide Mine Wastes. Mineral Association of Canada - Short Course Series* 22:271-292.
- Brandt, F., Bosbach, D., Krawczyk-Bärsch, E., Arnold, T., Bernhard, G. 2003. Chlorite dissolution in the acid pH-range: A combined microscopic and macroscopic approach. *Geochimica et Cosmochimica Acta* 67 (8):1451–1461.
- Cravotta, C.A., Brady, K., Smith, M.W., Beam, R.L. 1990. Effectiveness of the addition of alkaline materials at surface coal mines in preventing or abating AMD: part 1. Geochemical considerations. In: *Proceedings of the 1990 mining and reclamation conference and exhibition*, vol 1, WV Univ., Morgantown, p 221–225.
- Dold, B., Fontboté, L. 2001. Element cycling and secondary mineralogy in porphyry copper tailings as a function of climate, primary mineralogy and mineral processing. *Journal of Geochemical Exploration* 74:3-55.
- Dold, B. 2003. Speciation of the most soluble phases in a sequential extraction procedure adapted for geochemical studies of copper sulphide mine waste. *Journal of Geochemical Exploration* 80:55-68.
- Dold, B. 2010. Basic Concepts in Environmental Geochemistry of Sulfidic Mine-Waste Management. In: Kumar, E.S. (Ed.) *Waste Management*. InTech: <http://www.intechopen.com/articles/show/title/basic-concepts-in-environmental-geochemistry-of-sulfidic-minewaste-management>.

- Ferguson, K., Morin, K. 1991. The prediction of acid rock drainage lessons from the data base. In: *Proceedings of the second international conference on the abatement of acidic drainage*, vol.3, CANMET, Ottawa, p 83–106.
- Grano, S. 2009. The critical importance of the grinding environment on fine particle recovery in flotation. *Minerals Engineering* 22, 4:386-394.
- Holmström, H., Ljungberg, J., Ekström, K., Öhlander, B. 1999. Secondary copper enrichments in tailings at the Laver mine, northern Sweden. *Environmental Geology* 38:1-16.
- Hakkou, R., Benzaazoua, M., Brussiere, B. 2008. Acid Mine Drainage at the Abandoned Kettara Mine (Morocco): 1. Environmental Characterization. *Mine Water and the Environment* 27:145-159.
- Jambor, J.L. 1994. Mineralogy of sulphide rich tailings and their oxidation products. In: Jambor, J.L., Blowes, D.W. (Eds.) *Environmental Geochemistry of Sulfide Mine Wastes. Mineral. Assoc. Can. Short Course Ser.* 22:59-102.
- Junta de Andalucía. 2004. *Estudio de Elementos Traza en Suelos de Andalucía*. Serie Informes, Estudios, Trabajos y Dictámenes. Consejería de Medio Ambiente de la Junta de Andalucía, Sevilla, p 165.
- Kabata-Pendias, A., Pendias, H. 1992. *Trace elements in soils and plants*, 2nd ed., CRC, press, Boca Raton FL.
- Kloke, A. 1979. Contents of Arsenic, Cadmium, Chromium, Fluorine, Lead, Mercury, and Nickel. In: *Plants Grown on Contaminated Soil. UNECE Symposium*, Geneva.
- McGregor, R.G., Blowes, D.W. 2002. The physical, chemical and mineralogical properties of three cemented layers within sulphide-bearing mine tailings. *Journal of Geochemical Exploration* 76:195-207.
- Moncur, M.C., Ptacek, C.J., Blowes, D.W., Jambor, J.L. 2005. Release, transport and attenuation of metals from an old tailings impoundment. *Applied Geochemistry* 20:639–659.
- Paktunc, D., Dutrizak, E. 2003. Characterization of arsenate for sulphate substitution in synthetic jarosite using X-ray diffraction and X-ray absorption spectroscopy. *The Canadian Mineralogist* 41:905-919.
- Parvainen, A. 2009. Tailings Mineralogy and Geochemistry at the abandoned Haveri Au–Cu Mine, SW Finland. *Mine Water and the Environment* 28:291-304.
- Robertson, W.D. 1994. The physical hydrogeology of mill-tailings impoundments. In: Jambor, J.L., Blowes, D.W. (Eds.) *Environmental Geochemistry of Sulfide Mine Wastes. Mineral Association of Canada - Short Course Series* 22:1- 17.
- Savage, K.S., Bird, D.K., O'Day, P.A. 2005. Arsenic speciation in synthetic jarosite. *Chemical Geology* 215:473-493.
- Sidenko, N.V., Bortnikova, S.B.B., Lazareva, E.V., Kireev, A.D., Sherriff, B.L. 2005. Geochemical and mineralogical zoning of high-sulphide mine waste at the Berikul Mine-site, Kemerovo Region, Russia. *The Canadian Mineralogist* 43:1141-1156.
- Sidenko, N.V., Khozhina, E.I., Sherriff, B.L. 2007. The cycling of Ni, Zn, Cu in the system "mine tailings-ground water-plants": A case study. *Applied Geochemistry* 22:30-52.
- Sobek, A.A., Shuller, W.A., Freeman, J.R., Smith, R.M. 1978. Field and laboratory methods applicable to overburdens and minesoils. EPA Report EPA600/2-78-054. US EPA, Cincinnati.
- Thornthwaite, W., Mather, J.R. 1955. The water balance. *Publications in climatology* VIII(1). Laboratory of Climatology, Centerton, p 104.
- Thornthwaite, W., Mather, J.R. 1957. Instructions and tables for the computing potential evapotranspiration and the water balance. *Publications in climatology* X(3). Laboratory of Climatology, Centerton, p 311.
- Tornos, F., Inverno, C., Casquet, C., Mateus, A., Ortiz, G., and Oliveira, V. 2004. Metallogenic evolution of the Ossa Morena Zone. *Journal of Iberian Geology* 30:143-180.
- Vázquez, F. 1972. Génesis de la Mina María Luisa, La Nava (Huelva). Una mineralización zonada. *Boletín Geológico y Minero* 83(4): 377-386.
- Walsh, J.N., Gill, R., Thirlwall, M.F. 1997. Dissolution procedures for geological and environmental samples. In: Gill, R. (Ed.), *Modern Analytical Geochemistry. An Introduction to Quantitative Chemical Analysis Techniques for Earth, Environmental and Materials Scientists*. Longman, Essex England, 29–40.